

Correlation analysis between key volatile compounds and core functional bacterial community during Sichuan black tea processing

Si-yu Liao^a, Shuang Yang^a, Bin-lin Li^a, Xue Xia^a, Wen-bao Jia^a, Yi-qiao Zhao^a, Ling Lin^a, Jin-lin Bian^a, Tunyaluk Bouphun^{b,*}, Wei Xu^{a,*}

^a College of Horticulture, Tea Refining and Innovation Key Laboratory of Sichuan Province, Sichuan Agricultural University, Chengdu 611130, China

^b Faculty of Science and Agricultural Technology, Rajamangala University of Technology Lanna Lampang, Lampang 52000, Thailand

ARTICLE INFO

Keywords:

Black tea processing
Key volatile compounds
Core functional bacteria
Correlation relationship
Function prediction

ABSTRACT

Microorganisms participate in the transformation of non-volatile compounds during black tea processing, while their effects on aroma remains unclear. In the present study, 132 KVCs (key volatile compounds) were identified in Sichuan black tea (SBT), of which, linalool and p-cymene were responsible for the citrus-like and sweet aroma of SBT. During the processing of SBT, *Methylobacterium-Methylorubrum*, *Allorhizobium-Neorhizobium-Pararhizobium-Rhizobium*, *Pedobacter*, *Acidovorax*, and *Sphigomonas* were the dominant bacterial genera. PCoA (principal components analysis) and Anoism (analysis of similarities) indicated that the bacterial community undergone subtle changes in various processes. Additionally, *Pedobacter* and *Sphigomonas*, core functional bacteria contributing to SBT aroma formation, act mainly by secreting enzymes related to amino acid conversion and glycoside hydrolysis. These enzymes include kynureninase, L-cysteate sulfo-lyase, homoserine dehydrogenase, serine/threonine protein phosphatase 1, and aminotransferase. Overall, these findings provide a deep insight into the potential mechanism of aroma formation under bacterial influence during SBT processing.

1. Introduction

Black tea, a healthy beverage with high yield, is well-loved by consumers for its sweetness and charming aroma. Aroma is an important sensory index reflecting the quality of black tea, which consists of volatile compounds with variable contents and proportions (Z. Yang et al., 2013). Due to the differences in tea cultivars and processing technique, the flavor characteristics of Chinese black tea varies. For instance, Keemun black tea possesses a rose-like aroma, Xinyang black tea speaks a honey sugar-like aroma, while Sichuan black tea (SBT) produced in Sichuan province has a sweetness and citrus-like aroma (Jiang et al., 2023). A previous study has revealed that the key substances contributing to the aroma of SBT were linalool, p-cymene, and 3,7-dimethyl-1,5,7-octatrien-3-ol (Jiang et al., 2023). However, studies focused on the relationship between the core functional bacteria and flavor formation during SBT processing are rare, which hinders the

comprehensive elucidation of aroma formation mechanism of SBT to some extent.

The dominant processing steps of SBT are withering, rolling, fermentation, and drying. The processing technique is critical for SBT aroma formation. Enzymatic reaction related to the hydrolysis of volatile compounds precursors are main assistance for aroma formation (Huang et al., 2022). The degradation of glycosidic aroma precursors catalyzed by β -glucosidase and β -primeverosidase has been considered as the key force in aroma formation (Liang et al., 2023). However, it has been found that microorganisms play an important role in dynamic changes and the formation of quality characteristics during black tea processing, which differs from what has been understood about the mechanism of black tea quality formation (Jia et al., 2022; Liu, Lin, et al., 2023; Nurmilah et al., 2022; Tong et al., 2021). Additionally, microorganisms have been considered as a key factor affecting the “rock flavor” in Wuyi rock tea (Wu et al., 2024). Therefore, we speculate that

Abbreviations: SBT, Sichuan black tea; rOAV, relative odor activity value; HS-SPME-GC-MS, headspace solid-phase microextraction gas chromatography-mass spectrometry; KVCs, key volatile compounds; PICRUST2, phylogenetic investigation of communities by reconstruction of unobserved states 2; FTL, fresh tea leaves; WLA, leaves withered for 3 h; WLB, leaves withered for 6 h; RL, rolling leaves; FLA, leaves fermented for 1 h; FLB, leaves fermented for 2 h; FLC, leaves fermented for 3 h; BT, dried black tea; PCR, polymerase chain reaction; ASVs, amplicon sequence variants; OTUs, operational taxonomic units; PCA, principal component analysis; ANOVA, analysis of variance; PCoA, principal coordinates analysis; Anosim, analysis of similarities; RI, retention index.

* Corresponding authors.

E-mail addresses: Tunyaluk@rmul.ac.th (T. Bouphun), xuweianti@sicau.edu.cn (W. Xu).

<https://doi.org/10.1016/j.fochx.2024.101969>

Received 10 September 2024; Received in revised form 3 November 2024; Accepted 3 November 2024

Available online 5 November 2024

2590-1575/© 2024 The Authors. Published by Elsevier Ltd. This is an open access article under the CC BY-NC-ND license (<http://creativecommons.org/licenses/by-nc-nd/4.0/>).

the sweetness and citrus-like aroma of SBT may be related to the dynamic changes of bacterial community.

Volatile compounds are responsible for black tea aroma, and hundreds of volatile compounds, including alcohols, aldehydes, esters, and ketones, have been detected in black tea (Y. Yang, Xie, et al., 2024). The widely targeted volatileomics has been used for systematically study of active-aroma compounds in SBT (Jiang et al., 2023). However, few studies has been conducted on the relationship between active aromatic compounds and bacterial communities during processing and the core functional bacteria for SBT aroma formation.

Therefore, in this study, headspace solid-phase microextraction gas chromatography–mass spectrometry (HS-SPME-GC–MS) and 16S rRNA sequencing were employed to investigate the dynamics of aromatic compounds and bacterial communities during the processing of SBT, respectively. The key volatile compounds (KVCs) for the formation of SBT aroma were identified, and the core functional bacteria contributing to SBT aroma were clarified by analyzing the relationship between bacteria and KVCs. Furthermore, we revealed the potential mechanism of bacterial in SBT aroma formation in conjunction with the results of phylogenetic investigation of communities by reconstruction of unobserved states 2 (PICRUST2). Taken together, our study deepens the understanding of aroma formation mechanism during SBT processing.

2. Material and methods

2.1. Samples preparation

Fresh leaves (one bud and two leaves) of ‘Fuding dabaicha’ (*Camellia sinensis* (L.) O. Kuntze) were harvested for processing SBT in Sichuan province, China. The manufacture was as follows: aeration withering of fresh tea leaves (6 h), rolling (at 30 r/min for 2 h), fermentation (temperature: 40 °C, humidity: 95 %, 3 h), drying (initial drying for 10 min at 110 °C, cooling for 30 min at room temperature, re-drying for 120 min at 70 °C until the water content was 5 %).

During the processing, the fresh tea leaves (FTL), leaves withered for 3 h (WLA) and 6 h (WLB), rolling leaves (RL), leaves fermented for 1 h (FLA), 2 h (FLB), and 3 h (FLC), and dried black tea (BT) were collected separately. Samples from independent parallel batches were collected, and three replications were considered. All these samples were frozen by liquid nitrogen, and stored at –80 °C until use.

2.2. Identification of volatile compounds in SBT

2.2.1. Extraction of volatile compounds by HS-SPME

Samples were powdered in liquid nitrogen. 500 mg tea powder were mixed with 20 µL (10 µg/mL) internal standard (3-Hexanone-2,2,4,4-d₄, Merck kgaa, Germany) and NaCl (Sinopharm Co, China) saturated solution and were transferred into a 20 mL head-space vial (Agilent, Palo Alto, CA, USA). Subsequently, the sealed vials were equilibrated at 60 °C for 5 min, and a 120 µm DVB/CAR/PDMS fiber (Agilent) was exposed to the headspace at 60 °C for 15 min. The fiber was aged at 250 °C for 5 min before sampling.

2.2.2. Qualitative and quantitative analysis by GC–MS

The fiber was desorbed at injection port (250 °C for 5 min) and analyzed by GC–MS. The Agilent 7890B GC and a 7000D mass spectrometer (Agilent) equipped with a 30 m × 0.25 mm × 0.25 µm DB-5MS (5 % phenyl-polymethylsiloxane) capillary column (Agilent, J&W Scientific, Folsom, CA, USA) was used for GC–MS analysis. Temperature programs were as follows: initial oven temperature was 40 °C for 3.5 min, then raised to 100 °C at 10 °C/min, increased to 180 °C at 7 °C/min, and finally ramped to 280 °C at 25 °C/min, keep for 5 min. Helium (purity >99.999 %) was used as the carrier gas at a constant flow of 1.2 mL/min. The injection port temperature, injection mode, and solvent delay was 250 °C, spitless mode, and 3.5 min, respectively. The mass spectrometer was operated in electron impact (EI) ionization mode at

70 eV. The temperature of the ion source, quadrupole, and mass spectrometry interface was 230 °C, 150 °C, and 280 °C, separately. The selected ion monitoring (SIM) mode was used for the qualitative and quantitative of volatile compounds.

Original data of mass spectrometry was analyzed by using MassHunter software. All volatile compounds were identified in Metware database. Retention index (RI) was applied to further identification of compounds. Quantification was performed based on internal standard peak areas.

2.3. Identification of odor activity values of volatile compounds

The rOAV of volatile compounds was calculated using the ratio of the relative concentration to the odor threshold in water. Volatile compounds with rOAVs >1 were generally considered to greatly contribution to the aroma characteristics (M.-Q. Wang et al., 2020). The odor thresholds of volatile compounds were referred to a recent report (Huang et al., 2022).

2.4. Dynamic changes and function prediction of bacterial community

2.4.1. Total DNA extraction, amplification, and sequencing

The 16S rRNA high-throughput sequencing was used to analysis the composition and variation of the bacterial community. The total DNA of bacteria was extracted using the Qubit dsDNA HS Assay Kit (Q32854, Invitrogen, Life Technologies Inc. USA) according to the instructions. Primers used for PCR were as follows: the V3-V4 region of 16S rRNA gene was amplified using forward primer 341F (5'-CCTACGGGNGGCWGCAG-3') and reverse primer 805R (5'-GAC-TACHVGGGTATCTAATCC-3') (Logue et al., 2016). Throughout the whole process, ultrapure water was used instead of a sample solution, which aimed to exclude the possibility of false-positive PCR results as a negative control. The purification and quantification of PCR products were achieved through AMPure XT beads (Beckman Coulter Genomics, Danvers, MA, USA) and Qubit (Invitrogen, USA), respectively. Then amplicon pools were applied to sequence. Agilent 2100 Bioanalyzer (Agilent, USA) and the Library Quantification Kit for Illumina (Kapa Biosciences, Woburn, MA, USA) were utilized to assess the size and quantity of the amplicon library, individually. The libraries were sequenced on NovaSeq PE250 platform.

2.4.2. Sequence processing and data analysis

As we reported previously, bacteria were sequenced by an Illumina NovaSeq platform according to manufacturer's recommendations provided by LC-Bio (Jia et al., 2022). Paired-end reads were assigned to samples based on their unique barcode and truncated by cutting off the barcode and primer sequence, then merged by FLASH (v1.2.8). According to the fqtrim (v0.94), quality filtering on the raw reads was performed under specific filtering conditions to obtain high-quality clean tags. And chimeric sequences were filtered by Vsearch software (v2.3.4). Then we acquired feature table and feature sequences after dereplication using DADA2. The raw reads were removed joint and barcode sequence, and then the splicing, filtering, and denoising of raw data were sequentially completed through cutadapt (v1.9), FLASH (v1.2.8.), fqtrim (v0.94), Vsearch (v2.3.4.), and DADA2. Alpha diversity and beta diversity were calculated by normalizing to the same sequences randomly. Alpha diversity was applied in analyzing the complexity of species diversity for the sample, including shannon, simpson, chao 1, observed species, goods_coverage, and pielou_e. QIME2 was used to calculate all indices of alpha diversity and beta diversity. Then feature abundance was normalized using relative abundance of each sample according to SILVA (Release 138, <https://arb-silva.de/documentation/release138/>) classifier. Then the annotation of feature sequences was done through sequence alignment by Blast (<https://blast.ncbi.nlm.nih.gov/Blast.cgi>) and NT-16S database in SILVA database for each representative sequence. The resulting sequences were clustered into ASVs

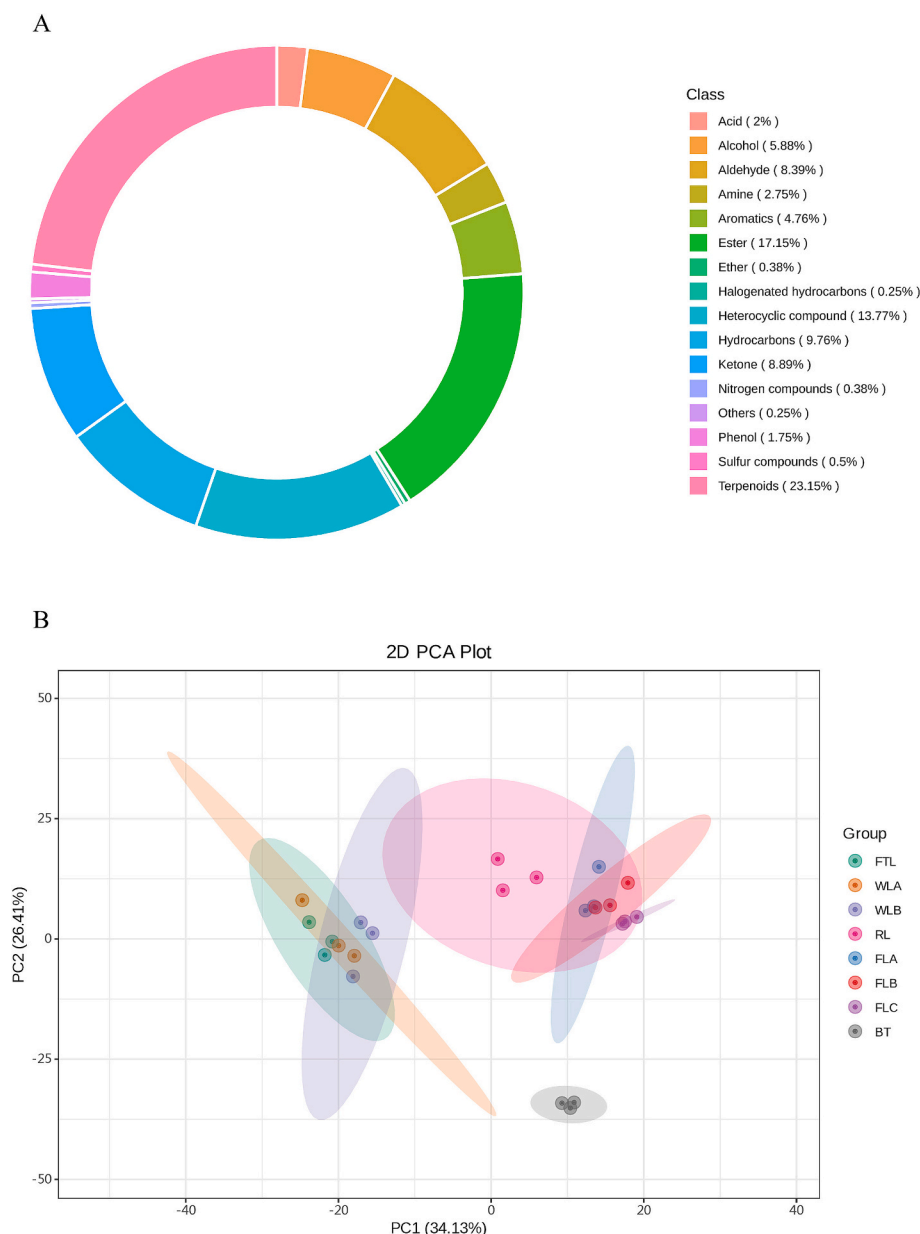


Fig. 1. The diagram of metabolite category composition (A) and PCA (B) from different processing stages of Sichuan black tea.

(amplicon sequence variants), a clustering method with high-precision species resolution for 16S rRNA analysis.

2.4.3. Function prediction by PICRUSt2

PICRUSt2 (<https://github.com/picrust/picrust2>) was a tool for predicting bacterial functions of bacteria in SBT processing. STAMP was used to display the significantly different gene function ranking results between bacterial community of different sample groups (t -test, $p < 0.05$).

2.5. Statistical analysis

Principal component analysis (PCA) and analysis of variance analysis (ANOVA) of volatile compounds was performed using R package (v4.1.2). The ANOVA results was shown as p -value. Alpha and beta diversity of bacterial community was drawn by R package (v3.5.2). Differences in bacterial community were analyzed based on bray curtis distance matrix, principal coordinates analysis (PCoA) and analysis of similarities (Anosim) similarity. OmicStudio tools (<https://www.omicstudio.cn/tool>)

was used to investigate the relationships between the relative contents of key volatile compounds and the top 30 (relative abundance) bacterial community.

3. Results and discussion

3.1. Dynamic changes of volatile compounds during SBT processing

As depicted in Fig. 1, a total of 799 volatile compounds were examined, including terpenoids (23.15 %), ester (17.15 %), heterocyclic compound (13.77 %), hydrocarbons (9.76 %), ketone (8.89 %), aldehyde (8.39 %), and alcohol (5.88 %) (Fig. 1A). The contribution rate of the first and the second principal component principal component (PC1 and PC2) were 34.13 % and 26.41 %, respectively, and the confidence level of whole samples was within 95 % (Fig. 1B). Besides, the discrepancy in composition of volatile compounds was distinct in different stages, with the samples in BT group significantly different from those in other groups (Fig. 1B). This indicated that drying played a critical role in SBT aroma formation (Jiang et al., 2023). Furthermore,

Table 1
Quantitation and relative odor activity values (rOAV) of key volatile compounds in Sichuan black tea.

No.	Compounds	CAS	RI	Content ± SD (μg/kg)	Threshold (μg/L)	Odor descriptions	rOAV
<i>Aldehyde</i>							
1	6-Nonenal, (Z)-	2277-19-2	1103.52	3.40 ± 0.15	0.00014	green, cucumber, melon, cantaloupe, honeydew, waxy, vegetable, orris, violet, leafy	24,273.63
2	(Z, Z)-3,6-Nonadienal	21,944-83-2	1100.00	0.91 ± 0.12	0.00005	fatty, soapy, cucumber	18,159.80
3	2-Nonenal, (E)-	18,829-56-6	1161.21	0.29 ± 0.02	0.00008	fatty, green, cucumber, aldehydic, citrus	3633.95
4	4-Heptenal, (Z)-	6728-31-0	900.00	0.08 ± 0.00	0.000025	oily, fatty, green, dairy, milky, creamy	3144.09
5	BenzeneacetAldehyde	122-78-1	1045.60	16.12 ± 0.75	0.0063	floral, honey, rose, cherry	2559.08
6	2,6-Nonadienal, (E,Z)-	557-48-2	1154.75	0.02 ± 0.00	0.00001	cucumber, green	1804.46
7	2,4-Decadienal, (E,E)-	25,152-84-5	1320.08	0.07 ± 0.01	0.00007	dusty, waxy, oily, soapy	940.99
8	2-Nonenal	2463-53-8	1161.00	0.07 ± 0.00	0.0001	fatty, green, waxy, cucumber, melon	671.12
9	Nonanal	124-19-6	1105.03	0.58 ± 0.61	0.001	aldehyde, citrus, orange peel	575.00
10	2-Nonenal, (Z)-	60,784-31-8	1148.00	1.20 ± 0.10	0.0045	orris, fatty, waxy, cucumber	267.60
11	BenzAldehyde, 4-methoxy-	123-11-5	1259.75	0.04 ± 0.01	0.0002	sweet, powdery, mimosa, floral, hawthorn, balsamic	199.07
12	2-Hexenal, (E)-	6728-26-3	853.20	0.56 ± 0.13	0.0031	green, grassy	180.50
13	(E)-2-Decenal	3913-81-3	1263.00	0.75 ± 0.01	0.005	waxy, fatty, earthy, green, cilantro, mushroom, aldehydic, fried, chicken, fatty, tallow	150.55
14	Heptanal	111-71-7	901.30	0.37 ± 0.02	0.0028	fresh, aldehydic, fatty, green, herbal, wine, ozonous	133.61
15	4-Nonenal, (E)-	2277-16-9	1105.00	0.26 ± 0.03	0.0022	fruity	119.56
16	Octanal	124-13-0	1003.28	0.06 ± 0.01	0.0007	lemon, citrus, green grass	91.43
17	Decanal	112-31-2	1206.43	0.01 ± 0.00	0.0001	sweet, aldehydic, waxy, orange peel, citrus, floral	85.54
18	2,6-Nonadienal, (E,E)-	17,587-33-6	1153.00	0.02 ± 0.00	0.0005	fresh, citrus, green, cucumber, melon	36.09
19	2-Hexenal	505-57-7	853.00	0.56 ± 0.13	0.0017	sweet, almond, fruity, green, leafy, apple, plum, vegetable	32.91
20	Hexanal	66-25-1	799.79	0.16 ± 0.01	0.005	aldehyde, grassy, green, leafy, vinegar	32.02
21	2-Undecenal, E-	53,448-07-0	1366.00	0.01 ± 0.00	0.00078	fresh, fruity, citrus, orange, peel	15.83
22	3-Hexenal, (Z)-	6789-80-6	800.00	0.03 ± 0.00	0.004	green, fatty, grassy, weedy, fruity, apple	8.46
23	BenzAldehyde	100-52-7	9621.46	2.31 ± 0.26	0.35	sweet, bitter, almond, cherry	6.59
24	cis-7-Decen-1-al	21,661-97-2	1212.00	0.01 ± 0.00	0.0022	citrus, aldehydic, cucumber	5.22
25	4-Heptenal	62,238-34-0	899.00	0.01 ± 0.00	0.0042	–	2.00
26	2-FurancarboxAldehyde, 5-methyl-	620-02-0	964.60	0.97 ± 0.06	0.5	spice, caramel, maple	1.94
27	2-Undecenal	2463-77-6	1367.00	0.01 ± 0.00	0.01	fresh, fruity, orange, peel	1.23
<i>Terpenoids</i>							
28	β-Ionone	14,901-07-6	1491	1.33 ± 0.06	0.00012	floral, woody, sweet, fruity, berry, tropical, beeswax	11,078.28
29	trans-.beta.-Ionone	79-77-6	1492.10	1.33 ± 0.06	0.0002	dry, powdery, floral, woody, orris	6646.97
30	(2S,4R)-4-Methyl-2-(2-methylprop-1-en-1-yl) tetrahydro-2H-pyran	3033-23-6	1110.00	0.37 ± 0.02	0.0002	rose, cortex, green, floral, geranium, powdery, metallic	1827.55
32	Linalool	78-70-6	1100.59	2.76 ± 0.27	0.006	floral, green	460.01
33	2-Methylisoborneol	2371-42-8	1198.00	0.22 ± 0.01	0.00048	earthy, musty	450.01
34	Naphthalene, 1,2,3,5,6,8a-hexahydro-4,7-dimethyl-1-(1-methylethyl)-, (1S-cis)-	483-76-1	1524.00	0.47 ± 0.04	0.00158	thyme, herbal, woody, dry	313.56
35	Cyclohexene, 1-methyl-4-(1-methylethylidene)-	586-62-9	1090.66	6.30 ± 0.38	0.2	citrus, pine	31.48
36	Bicyclo[2.2.1]heptan-2-ol, 1,7,7-trimethyl-, (1S-endo)-	464-45-9	1170.00	0.83 ± 0.06	0.048	pine, woody, camphor	17.32
37	trans-.beta.-Ocimene	3779-61-1	1049.00	0.52 ± 0.02	0.034	sweet, herbal	15.36
38	2-Buten-1-one, 1-(2,6,6-trimethyl-1,3-cyclohexadien-1-yl)-, (E)-	23,726-93-4	1386.00	0.02 ± 0.01	0.0015	apple, rose, honey, tobacco, sweet	14.87
39	D-Carvone	2244-16-8	1246.00	0.13 ± 0.01	0.01	spice, minty, bread, caraway	13.34
40	.alpha.-Irone	79-69-6	1526.00	0.02 ± 0.00	0.002	orris, floral, berry, violet, woody, powdery	10.44
41	2,4,6-Octatriene, 2,6-dimethyl-	673-84-7	1131.00	0.34 ± 0.01	0.034	sweet, floral, nut skin, peppery, herbal, tropical	9.91
42	2,4,6-Octatriene, 2,6-dimethyl-, (E,Z)-	7216-56-0	1131.00	0.34 ± 0.01	0.034	–	9.91
43	2,6-Octadien-1-ol, 3,7-dimethyl-, (Z)-	106-25-2	1230.47	0.29 ± 0.00	0.049	lemon, fresh	6.00
44	o-Cymene	527-84-4	1022.00	0.06 ± 0.00	0.0114	gasoline	5.11
45	Copaene	3856-25-5	1376.00	0.03 ± 0.00	0.006	woody, spicy, honey	4.85
46	endo-Borneol	507-70-0	1170.42	0.83 ± 0.06	0.18	pine, woody, camphor, balsamic	4.62
47	.beta.-Pinene	127-91-3	979.72	0.56 ± 0.04	0.14	dry, woody, resinous, pine, hay, green	3.98
48	Geranyl acetate	105-87-3	1384.01	0.12 ± 0.01	0.1	lemon	1.25

(continued on next page)

Table 1 (continued)

No.	Compounds	CAS	RI	Content \pm SD ($\mu\text{g}/\text{kg}$)	Threshold ($\mu\text{g}/\text{L}$)	Odor descriptions	rOAV
49	Citronellal	106-23-0	1154.55	0.07 \pm 0.00	0.06	sweet, dry, floral, herbal, waxy, aldehydic, citrus	1.08
<i>Ester</i>							
50	Butanoic acid, 3-methyl-, 2-phenylethyl ester	140-26-1	1491.00	0.06 \pm 0.00	0.00001	floral, fruity, sweet, rose, peach, apricot	6486.21
51	Benzoic acid, methyl ester	93-58-3	1097.75	0.49 \pm 0.06	0.00052	phenol, wintergreen, almond, floral, canga	947.39
52	2(5H)-Furanone, 3-hydroxy-4,5-dimethyl-	28,664-35-9	1110.00	1.82 \pm 0.15	0.011	extremely sweet, strong caramel, maple, burnt, sugar, coffee	165.90
53	Methyl salicylate	119-36-8	1200.00	4.47 \pm 0.28	0.04	caramel, peppermint	111.69
54	Propanoic acid, 2-methyl-, propyl ester	644-49-5	859.34	0.005 \pm 0.00	0.000086	sweet, ripe fruit, tropical, melon, berry	57.17
55	2(3H)-Furanone, 5-butyldihydro-	104-50-7	1261.00	0.44 \pm 0.02	0.0179	sweet, coconut, waxy, creamy, tonka, dairy, fatty	24.85
56	Methyl anthranilate	134-20-3	1348.51	0.04 \pm 0.00	0.003	fruity, grape, orange, flowery, neroli	12.82
57	Propanoic acid, 2-methyl-, 2-methylbutyl ester	2445-69-4	1016.00	0.12 \pm 0.00	0.014	fruity, ethereal, tropical, banana	8.64
58	Acetic acid, cyclohexyl ester	622-45-7	1043.00	0.01 \pm 0.00	0.0016	fruity, sweet, musty, ethereal	8.50
59	Propanoic acid, hexyl ester	2445-76-3	1108.00	0.05 \pm 0.00	0.008	pear, green, fruity, musty, rotten	6.76
60	Methyl jasmonate	1211-29-6	1638	0.02 \pm 0.01	0.003	floral, fresh, petal, magnolia, oily, waxy	5.74
61	Butanoic acid, 3-methyl-, phenylmethyl ester	103-38-8	1395.00	0.06 \pm 0.00	0.01	sweet, fruity, apple, pineapple, herbal	5.53
62	.delta.-Dodecalactone	713-95-1	1720.00	0.03 \pm 0.01	0.0076	peachy, oily, creamy, soapy	3.35
63	4-Decenoic acid, methyl ester, Z-	7367-83-1	1323.00	0.01 \pm 0.00	0.003	fruity, pear, mango, fishy, peach skin, green	2.93
64	cis-3-Hexenyl isovalerate	35,154-45-1	1238.00	0.06 \pm 0.01	0.02	fresh, green, apple, fruity, tropical, pineapple	2.90
65	Heptanoic acid, ethyl ester	106-30-9	1097.80	0.01 \pm 0.00	0.002	fruity, pineapple, cognac, rummy, wine	2.59
66	Cyclopentanecetic acid, 3-oxo-2-pentyl-, methyl ester	24,851-98-7	1665.06	0.02 \pm 0.00	0.013	floral, oily, jasmin, green, lactonic	1.90
67	Butanoic acid, 2-methyl-, hexyl ester	10,032-15-2	1236.00	0.03 \pm 0.00	0.022	green, waxy, fruity, apple, spicy, tropical	1.44
68	2,4-Decadienoic acid, ethyl ester, (E, Z)-	3025-30-7	1479.00	0.13 \pm 0.01	0.1	green, waxy, pear, apple, sweet, fruity, tropical	1.27
69	Butanoic acid, 2-methylpropyl ester	539-90-2	954.00	0.01 \pm 0.00	0.0094	sweet, fruity, pineapple, cherry, apple, overripe	1.16
70	3-Hexen-1-ol, acetate, (Z)-	3681-71-8	1006.92	0.03 \pm 0.00	0.031	fresh, green, sweet, fruity, banana, apple, grassy	1.02
<i>Heterocyclic compound</i>							
71	Pyrazine, 2-methoxy-3-(1-methylethyl)-	25,773-40-4	1097.00	1.40 \pm 0.08	0.000002	beany, chocolate, nutty	701,907.93
72	Pyridine, 2-pentyl-	2294-76-0	1202.00	11.73 \pm 0.64	0.0006	fatty, tallow, green, pepper, mushroom, herbal	19,549.46
73	2-Thiophenemethanethiol	6258-63-5	1105.00	0.27 \pm 0.02	0.00004	roasted, coffee, fishy	6694.32
74	Ethanone, 1-(2-thienyl)-	88-15-3	1092.00	6.53 \pm 0.51	0.001	sulfury, nutty, hazelnut, walnut	6528.65
75	Pyrazine, 2-ethyl-3,5-dimethyl-	13,925-07-0	1084.00	0.03 \pm 0.00	0.00004	burnt, almond, roasted, nutty, coffee	744.33
76	2-Furanmethanethiol, 5-methyl-	59,303-05-8	995.00	0.01 \pm 0.00	0.00005	sulfury, roasted, coffee	198.08
77	Furan, 2-pentyl-	3777-69-3	992.70	1.04 \pm 0.13	0.006	fruity, green, earthy, beany, vegetable, metallic	172.71
78	2(5H)-Furanone, 5-ethyl-	2407-43-4	966.00	0.89 \pm 0.02	0.0097	spice	92.03
80	2(4H)-Benzofuranone, 5,6,7,7a-tetrahydro-4,4,7a-trimethyl-, (R)-	17,092-92-1	1532.00	0.06 \pm 0.00	0.0021	musky, coumarin	29.50
81	trans-Linalool oxide (furanoid)	34,995-77-2	1075.24	4.67 \pm 0.31	0.19	floral	24.56
82	2-Furanmethanol, 5-ethenyltetrahydro-.alpha.,.alpha.,5-trimethyl-, cis-	5989-33-3	1074.00	4.67 \pm 0.31	0.32	earthy, floral, sweet, woody	14.58
83	Pyrazine, (2-methylpropyl)-	29,460-92-2	1074.00	3.47 \pm 0.14	0.4	green, vegetable, fruity	8.66
84	2H-Pyran-2-one, tetrahydro-6-methyl-	823-22-3	1095.14	0.20 \pm 0.00	0.0268	creamy, fruity, coconut	7.49
85	Ethanone, 1-(2-pyridinyl)-	1122-62-9	1034.00	0.50 \pm 0.11	0.1	popcorn, heavy, corn, chip, fatty, tobacco	4.98
86	Pyrazine, 3-ethyl-2,5-dimethyl-	13,360-65-1	1081.00	0.03 \pm 0.00	0.0086	potato, cocoa, roasted, nutty	3.46
87	5-Thiazoleethanol, 4-methyl-	137-00-8	1278.00	0.28 \pm 0.01	0.1	fatty, cooked, beefy, juice	2.79
88	Pyrazine, 2-methoxy-3-methyl-	2847-30-5	970.00	0.01 \pm 0.00	0.003	roasted almond, hazelnut, peanut	2.33
89	2-Acetyl-3-methylpyrazine	23,787-80-6	1082.00	0.04 \pm 0.00	0.02	nutty, flesh, roasted hazelnut, toasted grain, corn, chip, vegetable, nut skin, caramel	2.00
90	Pyrazine, 2-ethyl-5-methyl-	13,360-64-0	1005.00	0.03 \pm 0.00	0.016	coffee, beany, nutty, grassy, roasted	1.81
91	Benzothiazole	95-16-9	1228.00	0.10 \pm 0.00	0.08	meaty, vegetable, brown, cooked, beefy, coffee	1.30
<i>Ketone</i>							
92	1-Octen-3-one	4312-99-6	976.00	0.10 \pm 0.12	0.000005	mushroom	19,587.63
93	3,5-Octadien-2-one, (E,E)-	30,086-02-3	1073.00	1.48 \pm 0.13	0.0005	fruity, green, grassy	2967.23
94	5-Methyl-(E)-2-hepten-4-one	102,322-83-8	972.00	0.11 \pm 0.12	0.00005	hazelnut, nutty	2166.47
95	Cyclohexanone, 2,2,6-trimethyl-	2408-37-9	1036.00	0.16 \pm 0.00	0.0001	pungent, thujone, labdanum, honey, cistus	1584.99
96	2-Cyclopenten-1-one, 3-methyl-2-(2-pentenyl)-, (Z)-	488-10-8	1395.00	0.05 \pm 0.00	0.00026	woody, herbal, floral, spicy, jasmin, celery	195.76

(continued on next page)

Table 1 (continued)

No.	Compounds	CAS	RI	Content ± SD (μg/kg)	Threshold (μg/L)	Odor descriptions	rOAV
97	2-Cyclopenten-1-one, 2-hydroxy-3,4-dimethyl-	21,835-00-7	1075.00	2.72 ± 0.12	0.02	strong, caramel	136.04
98	1-(4-methylphenyl)-Ethanone	122-00-9	1183.00	0.39 ± 0.03	0.021	green, pea, bell pepper, galbanum	18.35
99	2-Butanone, 4-(2,6,6-trimethyl-2-cyclohexen-1-yl)-	31,499-72-6	1406.00	0.02 ± 0.00	0.0017	woody, floral, berry, orris, powdery, violet, raspberry, fruity	11.18
100	5,9-Undecadien-2-one, 6,10-dimethyl-, (E)-	3796-70-1	1453.00	0.06 ± 0.00	0.01	fresh, green, fruity, waxy, rose, woody, magnolia, tropical	5.66
101	5-Hepten-2-one, 6-methyl-	110-93-0	987.69	0.07 ± 0.01	0.05	herbal, green, citrus, musty, lemon grass	1.47
102	2-Butanone, 4-(2,6,6-trimethyl-1-cyclohexen-1-yl)-	17,283-81-7	1433.00	0.01 ± 0.00	0.0036	earthy, woody, mahogany, orris, dry, amber	1.42
103	4-Undecanone	14,476-37-0	1208.00	0.05 ± 0.00	0.041	fruity	1.23
104	Isophorone	78-59-1	1123.40	0.01 ± 0.00	0.011	cool, woody, sweet, green, camphor, fruity	1.09
<i>Aromatics</i>							
105	Benzene, 1-methyl-4-nitro-	99-99-0	1212.00	0.07 ± 0.00	0.003	–	22.03
106	2-Methoxy-4-vinylphenol	7786-61-0	1316.00	0.03 ± 0.00	0.003	spicy, raisin	10.05
107	Benzene, 1,4-diethyl-	105-05-5	1041.00	0.02 ± 0.00	0.0021	–	10.02
108	Naphthalene, 2-methyl-	91-57-6	1297.00	0.03 ± 0.00	0.004	sweet, floral, woody	7.14
109	Styrene	100-42-5	893.00	0.03 ± 0.00	0.0036	penetrating, balsamic, gasoline	7.10
110	Anethole	104-46-1	1287.00	0.08 ± 0.00	0.015	sweet, exotic, flowery, stewed	5.61
111	Naphthalene, 1-methyl-	90-12-0	1307.00	0.03 ± 0.00	0.008	camphor	3.57
112	p-Cymene	99-87-6	1025.99	0.02 ± 0.00	0.0114	woody, citrus	1.85
113	Benzene, nitro-	98-95-3	1080.00	0.26 ± 0.01	0.15	–	1.71
114	trans-Anethole	4180-23-8	1283.00	0.08 ± 0.02	0.057	sweet, anisic, licorice, mimosa	1.48
115	Estragole	140-67-0	1202.48	0.05 ± 0.01	0.035	sweet, sassafrass, anisic, spice, green, herbal, fennel	1.47
116	Benzene, 1,2,4,5-tetramethyl-	95-93-2	1115.00	0.11 ± 0.03	0.087	rancid, sweet	1.25
<i>Alcohol</i>							
117	1-Octen-3-ol	3391-86-4	979.76	0.02 ± 0.00	0.001	fatty, fruity, grassy, perfumy, sweet	18.84
118	2-Octen-1-ol, (E)-	18,409-17-1	1067.62	0.22 ± 0.01	0.02	green, citrus, vegetable, fatty	11.23
119	3,6-Nonadien-1-ol, (E,Z)-	56,805-23-3	1156.00	0.03 ± 0.01	0.003	fatty, green, cucumber, green pepper, fruity, watermelon	9.82
120	1-Octanol	111-87-5	1069.76	0.16 ± 0.01	0.022	intense citrus, rose	7.36
121	1-Nonanol	143-08-8	1170.64	0.04 ± 0.01	0.0053	fresh, clean, fatty, floral, rose, orange, oily	6.66
122	2-Nonanol	628-99-9	1099.20	0.13 ± 0.01	0.058	rose	2.20
123	3-Hexen-1-ol, (E)-	928-97-2	852.00	0.20 ± 0.01	0.11	green, privet, leafy, floral	1.86
124	Benzenemethanol, .alpha.-methyl-	98-85-1	1061.21	0.66 ± 0.02	0.479	fresh, sweet, gardenia, hyacinth	1.38
<i>Phenol</i>							
125	p-Cresol	106-44-5	1073.39	0.13 ± 0.01	0.00024	phenol, narcissus, animalic, mimosa	558.21
126	Phenol, 2,4-dichloro-	120-83-2	1171.00	0.06 ± 0.01	0.0014	–	41.53
127	Eugenol	97-53-0	1362.30	0.09 ± 0.01	0.0025	floral, clove	36.52
<i>Nitrogen compounds</i>							
128	Dodecanenitrile	2437-25-4	1490.00	0.01 ± 0.00	0.00009	citrus, orange, peel, metallic, spicy	81.83
<i>Sulfur compounds</i>							
129	Propanoic acid, 3-(methylthio)-	646-01-5	1092.92	0.06 ± 0.00	0.05	sweet, sulfury	1.23
<i>Acid</i>							
130	Benzeneacetic acid	103-82-2	1262.00	0.59 ± 0.08	0.135	sweet, honey, floral, honeysuckle, sour, waxy, civet	4.36
<i>Hydrocarbons</i>							
131	Tridecane	629-50-5	1300.00	0.12 ± 0.01	0.042	alkane	2.86
<i>Amine</i>							
132	BenzenAmine, N, N-dimethyl-	121-69-7	1101.00	0.08 ± 0.01	0.012	–	6.51

“–” indicated no relevant reports.

the PCA diagram indicated that the metabolites in fore-end processing were divided into three distinct classifications, with the first classification including FTL, WLA, and WLB, the second classification comprising RL, and the third classification covering FLA, FLB, and FLC (Fig. 1B). This suggests that rolling is a key procedure for the formation of SBT aroma.

The clustered heatmap of volatile compounds showed that these components were clustered into three categories. The first category of volatile compounds upregulated in BT, the second upregulated before rolling, whereas the third category upregulated during rolling and fermentation stages (Fig. S1). Compared to FTL, 28 volatile compounds appeared after processing, with 5, 5, 4, 4, 3, 3, 2, and 1 for ester, heterocyclic compounds, aldehyde, terpenoids, alcohol, ketone, aromatics, and amines, respectively (Fig. S1, Table S1). The contents of other compounds also changed, mainly induced by Maillard reaction, hydrolysis, oxidation, modification, and degradation (Yang, Wang, et al.,

2024).

Then we analyzed the rOAVs of the aroma substances and found that there were 132 components with rOAVs >1, which were considered to be the KVCs of SBT (Table 1). (Table 1). These KVCs consisted of aldehydes (27), terpenoids (22), esters (21), heterocyclic compounds (21), ketones (13), aromatics (12), alcohols (8), phenols (3), hydrocarbons (1), nitrogen compounds (1), sulfur compounds (1), and amine (1). Among these substances, 2-methoxy-3-(1-methylethyl)-pyrazine, (Z)-6-nonenal, 1-octen-3-on, 2-pentyl-pyridin, (Z, Z)-3,6-nonadiena, β-ionone, 2-thiophenemethanethiol, trans-.beta.-ionone, 1-(2-thienyl)-ethanone, and 3-methyl-(butanoic acid)-2-phenylethyl ester were also detected in other black teas (Sun et al., 2024; Yao et al., 2023).

SBT presented a sweet, floral, fruity, and citrus aroma. A previous study suggested that the citrus-like aroma is composed of linalool, p-cymene, and 3,7-dimethyl-1,5,7-octatrien-3-ol (Jiang et al., 2023). In this study, a total of 20 KVCs described as citrus-like odor were detected,

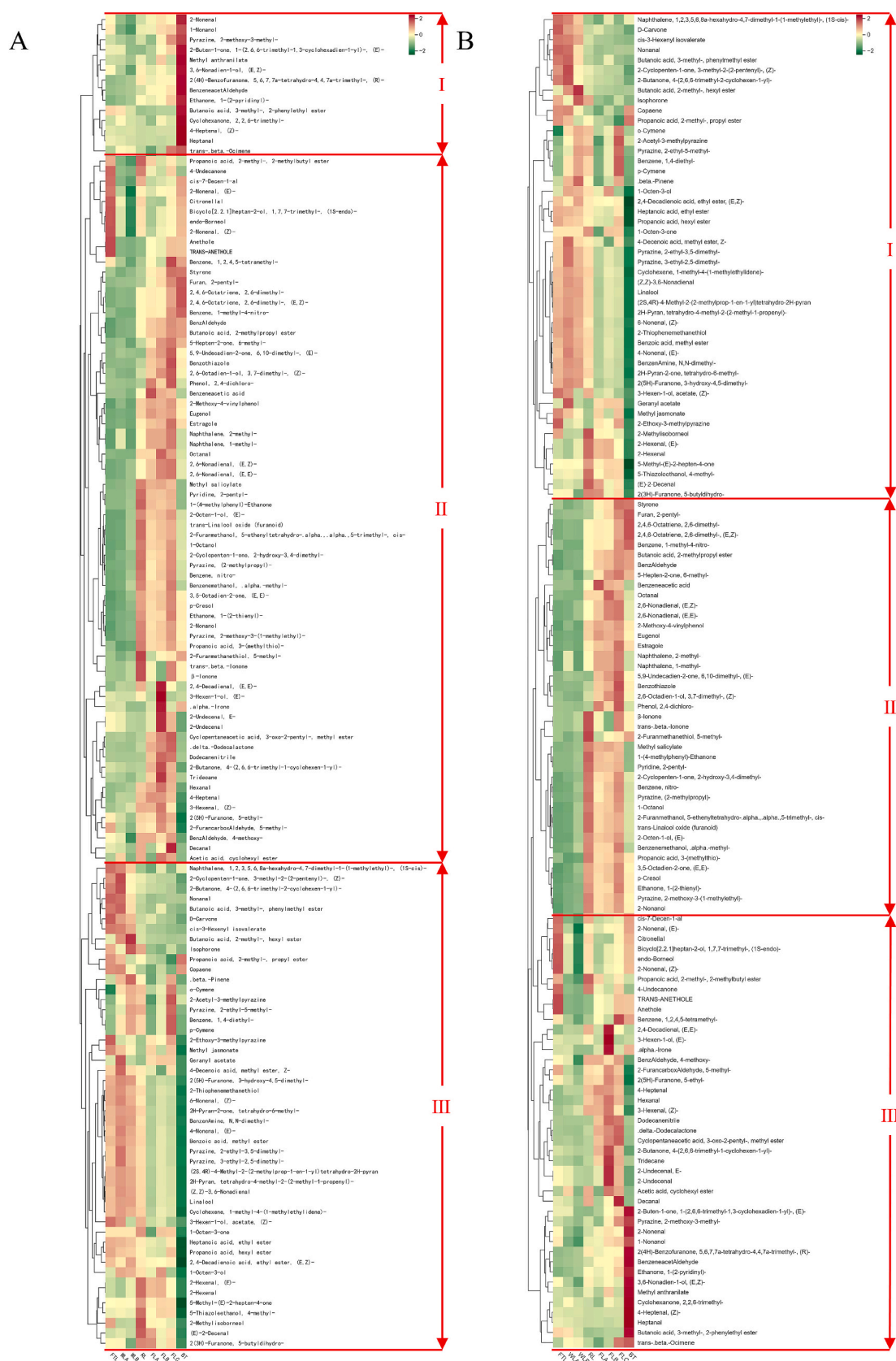


Fig. 2. Heatmap analysis of the relative contents (A) and rOAV (B) of the key volatile compounds in Sichuan black tea processing.

including (E)-2-nonenal, nonanal, (E)-2-decenal, octanal, decanal, dodecanenitrile, (E, E)-2,6-nonadienal, 1-methyl-4-(1-methylethylidene)-cyclohexene, (E)-2-undecenal, methyl anthranilate, (E)-2-octen-1-ol, 1-octanol, 1-nonanol, (Z)-3,7-dimethyl-2,6-octadien-1-ol, cis-7-decen-1-ol, p-cymene, 6-methyl-5-hepten-2-one, geranyl acetate, 2-undecenal, and citronellal (Table 1). We believed that the 20 KVCs with citrus-like odor were critical for the citrus-like aroma of SBT. Besides, we identified 23 KVCs with sweet-like odor in SBT, including 3-hydroxy-4,5-dimethyl-2(5H)-furanone, 2-hydroxy-3,4-dimethyl-2-cyclopenten-1-one, 2-methyl-(propanoic acid)-propyl ester, 2-hexenal, 5-butyldihydro-2(3H)-furanone, trans- β -ocimene, benzaldehyde, 5-methyl-2-furancarboxaldehyde, and so forth. Additionally, 26 KVCs with fruity-like odor and 27 KVCs with floral odor were found in BT, which may contribute to the formation of the flavor profile of SBT. All these KVCs interacted and influenced each other to form the complex aroma characteristics of SBT. Furthermore, combined with the previous study (Jiang et al., 2023), p-cymene and linalool were identified as the critical KVCs responsible for SBT aroma profile.

Clustered heatmap showed that these KVCs were divided into three categories. Specifically, the contents of the first category (14 kinds) were up-regulation in BT, the contents of the second category (70 kinds) were mostly up-regulation were ascending in RL, FLA, FLB, and FLC, while the third category (48 kinds) generally showed a higher content in FTL, WLA, and WLB (Fig. 2), and this is consistent with the PCA result.

Besides, the contents of KVCs with citrus-like, sweet, floral, and fruity odors had distinct variation pattern, with the highest relative content displayed after processing. Among the KVCs with citrus-like odor, cis-7-decen-1-ol, (E)-2-nonenal, citronellal, nonanal, 1-methyl-4-(1-methylethylidene)-cyclohexene, and geranyl acetate had the highest content before rolling; 1-octanol, (E)-2-decenal, and (E)-2-octen-1-ol had the highest contents after rolling stage; octanal, E-2-undecenal, 2-undecenal, decanal, dodecanenitrile, 6-methyl-5-hepten-2-one, (Z)-3,7-dimethyl-2,6-octadien-1-ol, (E, E)-2,6-nonadienal, and p-cymene were the most abundant in fermentation stage; 1-nonanol and methyl anthranilate presented the highest level in BT. For those with sweet odor, anethole, trans-anethole, 2-methyl-(propyl ester)-propanoic acid, 3-hydroxy-4,5-dimethyl-2(5H)-furanone, 3-methyl-(phenylmethyl ester)-butanoic acid, and tetrahydro-4-methyl-2-(2-methyl-1-propenyl)-2H-pyran were the highest before rolling; 2-hydroxy-3,4-dimethyl-2-cyclopenten-1-one, 3-(methylthio)-propanoic acid, 2-hexenal, (E)-2-decenal, and 5-butyldihydro-2(3H)-furanone were the most abundant after rolling; The highest levels of 5-methyl-2-furancarboxaldehyde, 4-methoxy-benzaldehyde, α -methyl-benzenemethanol, decanal, 2-acetyl-3-methylpyrazine, benzaldehyde, 2-(methylpropyl ester)-butanoic acid, benzenoacetic acid, estragole, benzenoacetic acid, and 2-methyl-naphthalene were found in the fermentation stage, while 1-nonanol and trans- β -ocimene were the highest in BT. Among the KVCs with floral odor, (Z)-2-Nonenal, anethole, (Z)-3-methyl-2-(2-pentenyl)-2-cyclopenten-1-one, methyl jasmonate, linalool, tetrahydro-4-methyl-2-(2-methyl-1-propenyl)-2H-pyran, and (2S, 4R)-4-methyl-2-(2-methylprop-1-en-1-yl)tetrahydro-2H-pyran were highest before rolling; trans-linalool oxide (furanoid), α -methyl-benzenemethanol, trans- β -ionone, cis- α -, α -5-trimethyl-5-ethenyltetrahydro-2-furanmethanol, and β -ionone were the most abundant after rolling; 2-(methylpropyl ester)-butanoic acid, (E)-6,10-dimethyl-5,9-undecadien-2-one, eugenol, (E)-3-hexen-1-ol, α -ionone, 3-oxo-2-pentyl-cyclopentaneacetic acid-methyl ester, benzenoacetic acid, 4-(2,6,6-trimethyl-1-cyclohexen-1-yl)-2-butanone, and 4-methoxy-benzaldehyde showed the highest level in fermentation stage; 2,6-dimethyl-2,4,6-octatriene, 2-nonenal, 1-nonanol, benzenoacetaldehyde, methyl anthranilate and (E)-1-(2,6,6-trimethyl-1.3-cyclohexadien-1-yl)-2-buten-1-one exhibited the highest content in BT. For KVCs with fruity odor, propenoic acid-2-methyl-2-methylbutyl ester, 4-undecanone, 3-methyl-butanoic acid-phenylmethyl ester, cis-3-hexenyl isovalerate, 2-methyl-butanoic acid-hexyl ester, Z-4-decenoic acid-methyl ester, (Z)-6-nonenal, (E)-4-nonenal, (Z)-3-hexen-1-ol-acetate, heptanoic acid-ethyl ester,

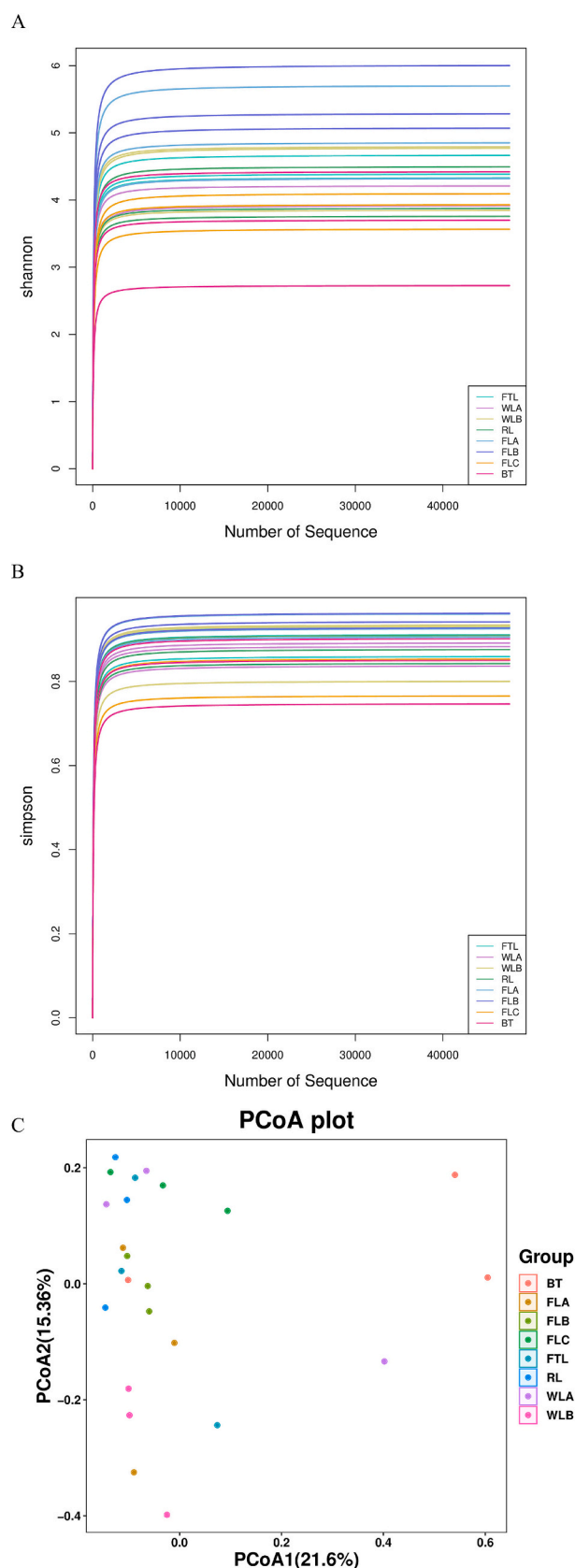


Fig. 3. Diversity of the bacterial community of samples in Sichuan black tea processing. Changes of bacterial community diversity in samples based on the rarefaction curve of Shannon index (A) and Simpson index (B) of alpha diversity. PCoA (C) was employed to reveal the changes in bacterial community diversity based on bray_curtis distance matrix of beta diversity.

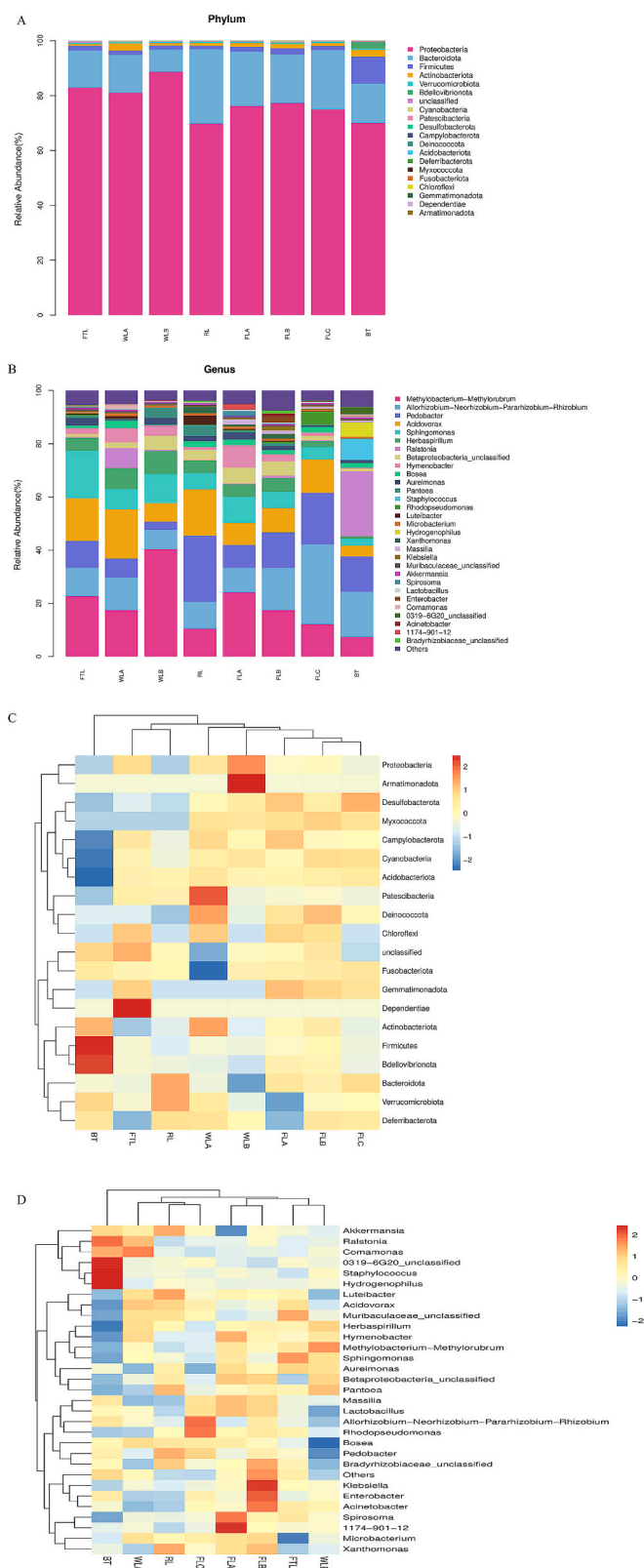


Fig. 4. Changes in the relative abundance of bacterial communities in Sichuan black tea processing. The stacked bar chart and heatmap of the relative abundance of bacterial communities at phylum level (A and C) and genus level (B and D).

propanoic acid-hexyl ester, tetrahydro-6-methyl-2H-pyran-2-one, and (E, Z)-2,4-decadienoic acid-ethyl ester were the most abundant before rolling stage; 2-hexenal exhibited the highest content after rolling procedure; 2-methylpropyl ester-butyanoic acid, (E, Z)-2,6-nonadienal, (E, E)-3,5-octadien-2-one, delta-dodecalactone, (Z)-3-hexenal, and acetic acid-cyclohexyl ester were the highest in fermentation stage; 2-nonenal, 1-nonanol, (E, Z)-3,6-nonadien-1-ol, 2-methyl-propanoic acid-propyl ester, 2-pentyl-furan, and heptanal were the most abundant in BT. Overall, the fermentation stage promoted the formation of KVCs with citrus-like, sweet, and floral odor, while the processing of SBT lead to the loss of KVCs with fruity odor. These results indicate that fermentation is a crucial stage for the content enhancement of these specific KVCs, while rolling and drying could drives changes in the composition of volatile compounds (Yang, Wang, et al., 2024).

Additionally, the rOAV clustering heatmap of KVCs showed that these KVCs were also classified into three categories (Fig. 2B). The rOAVs of the first category (48 kinds) were mostly up-regulation in FTL, WLA, and WLB, those in the second category (41 kinds) were mostly up-regulated in RL, FLA, FLB, and FLC, and those in the third category (43 kinds) were mainly up-regulated in BT. The relative content of KVCs and rOAVs showed similar trends throughout processing (Fig. 2). For KVCs with citrus-like odor, nonanal, 1-methyl-4-(1-methylethylidene)-cyclohexene, geranyl acetate, cis-7-decen-1-al, (E)-2-nonenal, and citronellal had the highest rOAVs before rolling; (E)-2-decenal, 1-octanol, and (E)-2-octen-1-ol possessed the highest rOAVs after rolling; The highest rOAVs values were found in p-cymene, 6-methyl-5-hepten-2-one, octanal, (E, E)-2,6-nonadienal, (Z)-3,7-dimethyl-2,6-octadien-1-ol, dodecanenitrile, E-2-undecenal, 2-undecenal, and decanal in the fermentation stage while 1-nonanol and methyl anthranilate had the highest rOAVs in BT. These results suggest that fermentation is a key procedure for the formation of the typical flavor profile of SBT, whereas rolling and drying lead to the dramatic fluctuation of volatile compounds via complex chemical reactions (Z. Chen et al., 2024). Specifically, rolling promoted the changes of relevant content of KVCs by disrupting leaf tissues, and thus leading to the formation of alcohol and aldehyde, while drying affected the contents of KVCs by means of high temperature (Z. Chen et al., 2024).

3.2. Variation of bacterial community during SBT processing

16S rRNA sequencing showed that 19 phyla, 39 classes, 92 orders, 173 families, 366 genera, and 626 species were detected in the SBT samples (Table S2). The α -diversity suggested that the bacterial diversity of FLB group was significantly higher ($p < 0.05$) than the samples from the other groups (Fig. 3A, Fig. 3B and Fig. S2). In the β -diversity analysis, the PCoA results showed that all samples were distributed in the first quadrant, with PC1 and PC2 contributing 21.60 % and 15.36 %, respectively (Fig. 3C). However, two samples in BT group were distant from the others, indicating that drying affect the diversity and composition of the bacterial community remarkably. In Anosim similarity analysis, the test statistic was 0.217 and the p -value was 0.003 (Table S2). The clusters identified by the β -diversity analysis were statistically significantly different ($p < 0.01$), yet the observable statistical differences between these groups were minor. In other words, the bacterial community undergone subtle changes during SBT processing, while the differences in bacterial community composition between different processes were minute.

The relative abundances of the top 20 bacteria for respective processing was presented in Table S3. The bacterial community composition observed in this study was different from that of previous researches (Jia et al., 2022; Liu, Lin, et al., 2023; Nurmilah et al., 2022; Ren et al., 2024; Tong et al., 2021), which may be caused by the differences in raw material, processing environment, manufacturing conditions, and so forth. As shown in Fig. 4A, *Proteobacteria* (69.78–88.68 %) was the main phylum in all samples, which was consistent with our previous study (Jia et al., 2022), followed by *Bacteroidota* (8.08–27.15 %) and *Firmicutes*

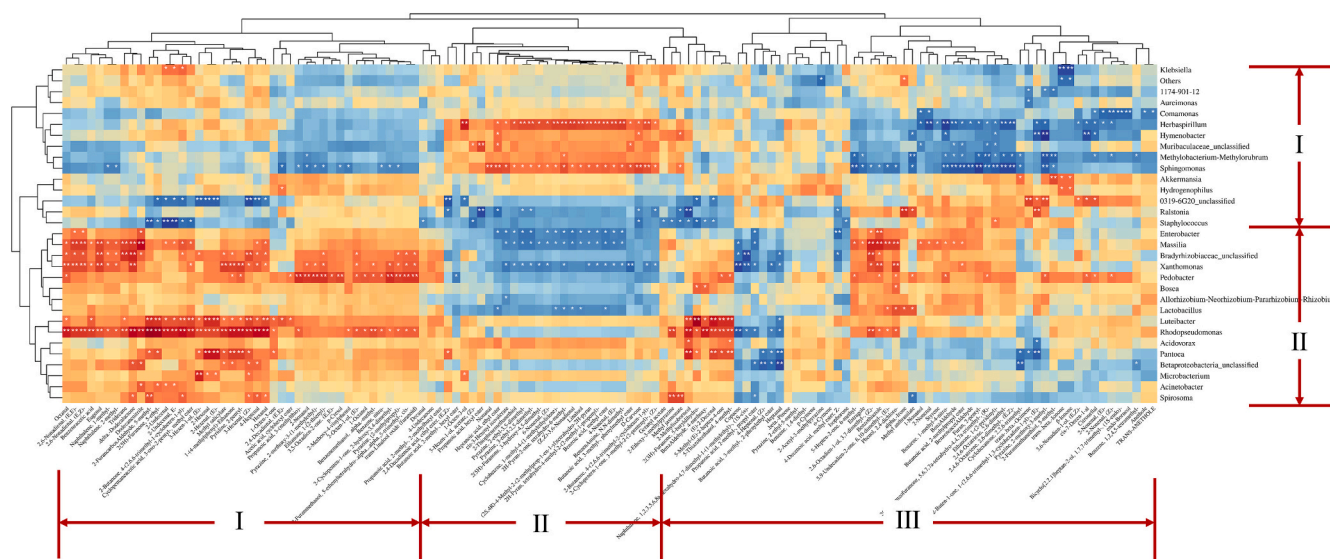


Fig. 5. Correlation heatmap analysis between key volatile compounds and bacterial communities with top 30 relative abundance during Sichuan black tea processing.

(1.21–9.88 %). On genus level, *Methylobacterium-Methylorubrum* (7.34–40.34 %), *Allorhizobium-Neorhizobium-Pararhizobium-Rhizobium* (7.20–29.87 %), *Pedobacter* (3.18–24.94 %), *Acidovorax* (3.99–18.58 %), and *Sphingomonas* (2.68–17.80 %) were dominant (Fig. 4B). Except for *Ralstonia* (24.52 %), the relative abundances of almost all dominant bacteria decreased in BT. Rolling and drying induced drastic changes in the composition of bacteria (Fig. 4B), which was attributed to the release of sterilizing substances like polyphenols in rolling stage and the high-temperature treatment during drying (Ren et al., 2024). And this is similar to the trend of relative KVC content during SBT processing. The relative abundance of *Methylobacterium-Methylorubrum* increased and reached the highest level in WLB, then decreased (RL), then increased again (FLA), and finally decreased again and reached a minimum in BT. Besides, as dominant bacteria in SBT processing, the relative abundances of *Allorhizobium-Neorhizobium-Pararhizobium-Rhizobium*, *Pedobacter*, *Acidovorax*, and *Sphingomonas* were the highest in FLC (29.87 %), RL (29.94 %), WLA (18.58 %), and FTL (17.80 %), respectively. Most of these dominant genera belonged to *Proteobacteria* phylum, and only *Pedobacter* genus belonged to *Bacteroidota* phylum (Fig. S3).

Clustering heatmap analysis showed that all samples were divided into two categories, one category was BT, and another category was the samples except for BT (Fig. 4C and Fig. 4D), which is the same as the results of PCoA. At phylum level, the relative abundance of *Deferentia*, *Patescibacteria*, *Proteobacteria* and *Armatimonadota*, *Firmicutes*, *Bdellovibrionota*, and *Actinobacteriota* increased in FTL, WLA, WLB, and BT, respectively. However, the relative abundance of bacteria at phylum level exert no significant fluctuation in RL and fermentation stages (Fig. 4C). At genus level, the relative abundances of *Sphingomonas*, *Muribaculaceae_unclassified*, *Comamonas* and *Methylobacterium-Methylorubrum* increased in FTL, WLA, and WLB samples, individually. Increased abundance of *Allorhizobium-Neorhizobium-Pararhizobium-Rhizobium*, *Rhodopseudomonas*, *Bradyrhizobiaceae_unclassified*, *Klebsiella*, *Enterobacter*, *Acinetobacter*, and *Spirosoma* was observed in the fermentation stage. Samples in BT group showed an increase in the abundance of *Akkermansia*, *Ralstonia*, *0319-6G20_unclassified*, *Staphylococcus*, and *Hydrogenophilus*. It is well known that withering is critical for the formation of black tea aroma (Huang et al., 2022), so changes of volatile compounds at this stage may be related to bacteria (*Patescibacteria*, *Proteobacteria*, and *Armatimonadota* at phylum level; *Comamonas* and *Methylobacterium-Methylorubrum* at genus level). Besides, both FLA and FLB were clustered at the phylum and genus levels, suggesting that the bacterial composition was stable in the early stages of

fermentation. In fermentation stage, tea polyphenols are oxidized to produce tea pigments, which may contribute to a consistent bacterial composition at this stage (Jia et al., 2022; Liu, Lin, et al., 2023; Tong et al., 2021). Furthermore, the relative abundance of bacteria in RL was declined mostly, which was attributed to the spillage of tea polyphenols during rolling (Ren et al., 2024).

Multiplicity populations of bacteria was associated with flavor profiles and health benefits of fermented foods (Qu et al., 2024). Additionally, bacteria affected the color, taste, and fragrance of Chinese dark tea (Liu, Li, et al., 2023). During black tea quality formation, dominant genera like *Sphingomonas*, *Methylobacterium*, and *Variovorax* were closely related to contents of tea polyphenols and their oxidation products. Of which, *Sphingomonas* was considered to be the key bacterium related to nonvolatile metabolites of black tea and exist on the surface of tea leaves (Nurmilah et al., 2022; Tong et al., 2021). The volatile compounds of black tea are generated from non-volatile compounds through a series of complex reactions during processing, so we hypothesize that these bacteria are critical for the formation of black tea aroma.

According to the annotation of NT-16S database, both *Methylobacterium* and *Methylorubrum* referred to *Methylobacterium* sp., a *Proteobacteria* phylum, rod-shaped and gram-negative. *Methylobacterium* was distributed in the phyllosphere area of tea plants and could secrete carotenoids to resist ultraviolet rays (Mo et al., 2023). Interestingly, carotenoids are linked to tea quality mainly by affecting the volatile compounds and appearance of black tea (Q. Chen et al., 2022). This indicates that *Methylobacterium* was beneficial for the aroma formation of SBT. Besides, *Methylobacterium* possess high L-methioninase activity and anticancer potential (Kavya & Nadumane, 2023), which is related to the health benefits of SBT. *Allorhizobium-Neorhizobium-Pararhizobium-Rhizobium* is annotated as *Rhizobium* genus in NT-16S database. *Rhizobium*, a genus of gram-negative and thermostability soil bacterium with nitrogen-fixing capacity, was stably detected during SBT processing and increased dramatically during the fermentation stage. This may be attributed to the ability of *Rhizobium* to secrete the activator homologous substances of protocatechuate catabolism (Parke, 1996), thus affecting the metabolism of phenolic compounds. Furthermore, *Pedobacter* was related to the production of hotrienol, epicatechin gallate, and theanine of Wuyi rock tea (Wu et al., 2024). *Acidovorax* was detected in black tea processing and participated in the chemical metabolism of tea, especially sugar metabolism (Liu, Lin, et al., 2023). Therefore, we considered that the bacterial community must play a key

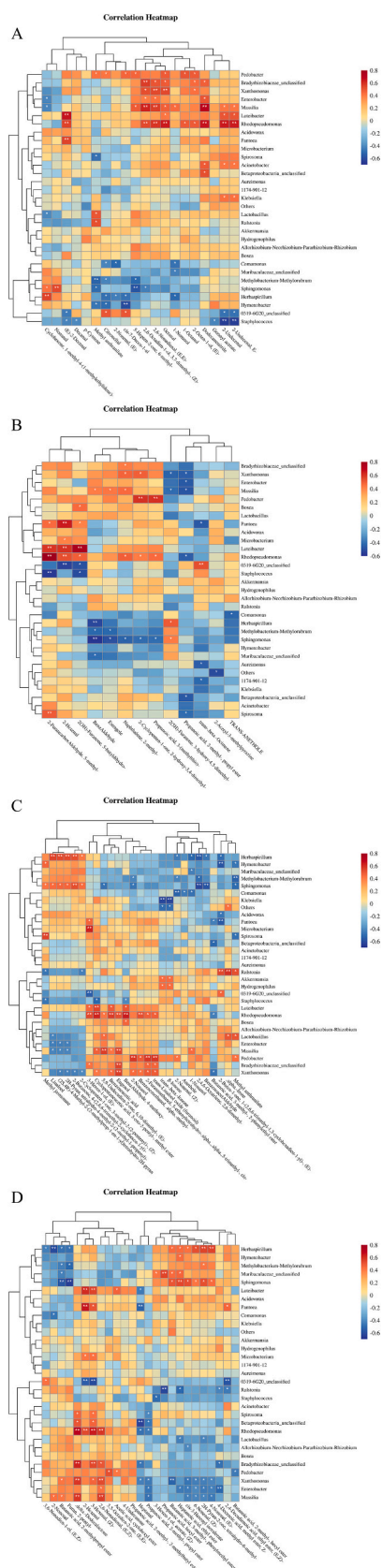


Fig. 6. Correlation heatmap analysis between bacterial communities with top 30 relative abundance and key volatile compounds with critical odor characteristics during Sichuan black tea processing.

role on the metabolism of volatile compounds during SBT processing.

3.3. Correlation analysis between KVCs and bacterial community

To investigate the potential correlation relationship between volatile compounds and bacterial community during SBT processing, we performed a correlation clustering heatmap analysis of KVCs and the bacteria with relative abundance in the top 30 (Fig. 5). The result showed that KVCs were clustered into three groups and bacteria were clustered into two groups. As shown in Fig. 5, *Pedobacter*, *Allorhizobium-Neorhizobium-Pararhizobium-Rhizobium*, and *Acidovorax* were positively correlated with KVCs in part I, overwhelmingly negatively related in part II, and partially positively correlated in part III. However, the correlation of *Methylobacterium-Methylorubrum* with KVCs was opposite to that of *Sphingomonas* with KVCs. This indicates that the bacterial community affects the composition of volatile compounds during SBT processing.

Furthermore, based on the odor descriptions presented in Table 1, we investigated the correlation between the content of KVCs with citrus-like, sweet, floral, and fruity odors and the relative abundance of bacteria by using correlation cluster heatmap analysis (Fig. 6). The results showed that these bacteria were significantly correlated with the KVCs exhibiting different odor ($p < 0.05$). *Methylobacterium-Methylorubrum* was significantly positively correlated with (E)-4-nonenal having a fruity-like odor, whereas negatively correlated with KVCs presenting citrus-like, sweet, and floral odors ($p < 0.05$). *Allorhizobium-Neorhizobium-Pararhizobium-Rhizobium* showed a significant negative correlation with cis-3-hexenyl isovalerate having fruity-like odor, while had no significant correlation with KVCs presenting citrus-like, sweet, and floral odors ($p < 0.05$). *Pedobacter* was significantly positively related with methyl anthranilate, citronellal, cis-7-decen-1-al, 6-methyl-5-hepten-2-one, octanol, 1-octanol, (E)-2-octen-1-ol, alpha-methyl-benzenemethanol, 2-hydroxy-3,4-dimethyl-2-cyclopenten-1-one, 3-(methylthio)propanoic acid, 2-Nonanol, alpha-methyl-benzenemethanol, cis-alpha.,alpha.-5-trimethyl-5-ethenyltetrahydro-2-furanmethanol, trans-Linalool oxide (furanoid), (Z)-2-nonenal, (E, E)-3,5-octadien-2-one, and acetic acid-cyclohexyl ester ($p < 0.05$). *Acidovorax* correlated negatively with (E)-1-(2,6,6-trimethyl-1.3-cyclohexadien-1-yl)-2-buten-1-one, which exhibits a floral odor, but had no significant correlation with these specific KVCs ($p < 0.05$). *Sphingomonas* was significantly positively correlated with 1-methyl-4-(1-methylenthylidene)-cyclohexene, nonanal, 3-methyl-(phenylmethyl ester)-butanoic acid, 3-hydroxy-4,5-dimethyl-2(5H)-furanone, tetrahydro-4-methyl-2-(2-methyl-1-propenyl)-2H-pyran, methyl jasmonate, linalool, (2S, 4R)-4-methyl-2-(2-methylprop-1-en-1-yl)tetrahydro-2H-pyran, tetrahydro-4-methyl-2-(2-methyl-1-propenyl)-2H-pyran, 4-(2,6,6-trimethyl-1-cyclohexen-1-yl)-2-butanone, (Z)-3-methyl-2-(2-pentenyl)-2-cyclopenten-1-one, heptanoic acid-ethyl ester, cis-3-hexenyl isovalerate, (Z)-6-nonenal, tetrahydro-6-methyl-2H-pyran-2-one, and (E)-4-nonenal ($p < 0.05$). Overall, *Methylobacterium-Methylorubrum* and *Allorhizobium-Neorhizobium-Pararhizobium-Rhizobium* were positively related with fruity-like odor, *Pedobacter* and *Sphingomonas* were positively contributed to citrus-like, sweet, floral, and fruity-like odor, while *Acidovorax* was positively associated with fruity-like odor. Besides, the KVCs with citrus-like and sweet odor were positively correlations with *Bradyrhizobiaceae_unclassified*, *Xanthomonas*, *Massilia*, *Luteibacter*, *Rhodopseudomonas*, *Pantoea*, *Herbaspirillum*, and *Spirosoma* ($p < 0.01$). As shown in Fig. 6, the genera of *Sphingomonas*, *Pedobacter*, *Rhodopseudomonas*, *Luteibacter*, *Bradyrhizobiaceae_unclassified*, *Xanthomonas*, *Massilia*, and *Herbaspirillum* may be closely related to the formation of SBT aroma characteristics, and these organisms could serve as core functional bacteria in SBT processing.

As reported previously, *Pantoea* was related to the metabolism of C₆ ~ C₉ aldehydes, alcohols, and fatty acids esters (A. Wang et al., 2024). A variety of bacteria have been reported to be involved in the formation of non-volatile compounds in black tea (Jia et al., 2022; Liu, Lin, et al.,



Fig. 7. Prediction of gene function in black tea samples from different processing stages based on the KEGG database [FTL vs WLB (A), RL vs WLB (B), RL vs FLC (C), FLC vs BT (D)]. P -value < 0.05.

2023; Tong et al., 2021). And the conversion of non-volatile compounds to volatiles was one of the main sources of aroma formation in black tea (Z. Chen et al., 2024). Therefore, the cooperation of bacteria communities influenced SBT aroma formation.

3.4. Functional prediction for bacterial community by PICRUST2

Functional prediction of the bacterial community during SBT processing showed that the adenosine deoxyribonucleotides de novo biosynthesis II was only expressed in FLA, FLB, FLC, and BT (Fig. S4), suggesting that microbial reproductive activity was vigorous during fermentation. The up-regulation of the adenosine deoxyribonucleotides de novo biosynthesis II and the superpathway of menaquinol family biosynthesis in BT might be attributed to the microbial colonisation caused by the increase in temperature during the drying process. In addition, the succinate fermentation to butanoate was just up-regulation in RL and butanoate existed in black tea aroma (Akiyama et al., 2012).

As shown in Fig. 7, synthesis, degradation, and transportation of compounds were constantly present throughout the process, indicating that bacterial metabolism was active in the entire process. The mean proportions of phospholipid-binding lipoprotein MlaA, transcription elongation factor GreB, and enzymes related to bacterial flagella formation were higher in FTL ($p < 0.01$), which is correlated with the high abundance of microorganisms in FTL. Amino acids can generate pleasant odors or act as precursors involved in flavor formation through Maillard reactions. The mean proportions of kynureninase, tryptophan 2,3-dioxygenase, and phenylalanine-4-hydroxylase was obviously high in FTL, which participated in the metabolism of tryptophan, phenylalanine, tyrosine, and alanine (Fitzpatrick, 2023; Iwamoto et al., 1995; Li & Fitzpatrick, 2013; Phillips et al., 2019; Thackray et al., 2008). These enzymes provided a material basis for aroma formation in the subsequent processes. The mean proportions of enzymes concerning amino acid transport and synthesis were significantly increased in WLB, indicating that withering is able to promote amino acid synthesis. Similarly, the mean proportions of enzymes involved in amino acids metabolism (kynureninase, L-cysteate sulfo-lyase, homoserine dehydrogenase, serine/threonine protein phosphatase 1, aminotransferase, glycine dehydrogenase, tyrosine phenol-lyase), increased in RL and FLC. Among these enzymes, kynureninase catalyses the hydrolysis of L-kynurenine to produce anthranilate and L-alanine in bacteria (Phillips et al., 2019). L-cysteate sulfo-lyase participates in the pyridoxal 5'-phosphate-coupled desulphonated reaction of L-cysteate (Denger et al., 2006). In microorganisms, aspartic acid was converted into homoserine and provides precursors for the biosynthesis of threonine, isoleucine, and methionine, thus homoserine dehydrogenase was involved in the biosynthesis of these amino acids at the second stage (Thomas et al., 1993). Serine/threonine protein phosphatase 1 and aminotransferase participated in the transmembrane transport of amino acids (Sabrialabed et al., 2020). Therefore, the up-relation of these enzymes in RL and FLC may lead to changes in the category and content of amino acids, ultimately leading to flavor variation of SBT.

Furthermore, the mean proportions of enzymes related to D-xylose transport system, L-gulonate 5-dehydrogenase, and rhamnosyltransferase subunit A increased in RL and FLC when compared with those in FTL and WLB. This indicates that microorganisms affected the hydrolysis reaction of glycosides, which is critical for the formation of black tea aroma.

The aforementioned results demonstrated that withering, rolling, and fermentation are the key stages of SBT aroma formation. In these stages, the expression levels of enzymes related to amino acids conversion and glycoside hydrolysis were up-regulated, which enhanced the content of aroma precursors such as amino acids, and consequently influenced flavor formation.

In the present study, the dynamic changes of bacterial community were consistent with flavor formation. We therefore concluded that the bacterial community affects flavor formation. Functional prediction

showed that the bacterial community affected metabolism of volatile compounds via secreting the enzymes related to amino acids conversion and glycoside hydrolysis, which in turn affected aroma formation. Simultaneously, different bacteria would work together to shape the flavor.

4. Conclusion

This study investigated the changes in volatile compounds and bacterial communities during the processing of SBT and revealed the correlation between them. The result showed that 132 KVCs presented the typical flavor of SBT, including linalool, benzeneacetaldehyde, β -ionone, methyl jasmonate, (Z)-3,7-dimethyl-2,6-octadien-1-ol, nonanal, 3-hydroxy-4,5-dimethyl-2(5H)-furanone, 2-hexenal, (E)-4-nonenal, and so forth. Linalool and p-cymene were identified as the source of citrus-like and sweet aroma of SBT. *Methylobacterium-Methylorubrum*, *Allo-rhizobium-Neorhizobium-Pararhizobium-Rhizobium*, *Pedobacter*, *Acidovorax*, and *Sphingomonas* were the dominant genera during SBT processing. The bacterial community, especially *Pedobacter* and *Sphingomonas*, were positively correlated with the content of KVCs in SBT. Functional prediction of bacteria suggested that the mean proportions of enzymes related to amino acids conversion and glycoside hydrolysis (kynureninase, L-cysteate sulfo-lyase, homoserine dehydrogenase, serine/threonine protein phosphatase 1, and aminotransferase) were highly increased in withering and fermentation stages, including. Overall, our study provides new insights into the dynamic changes of volatile compounds and bacterial community during SBT processing and deepens our understanding of the core bacteria in black tea.

CRediT authorship contribution statement

Si-yu Liao: Writing – original draft, Visualization, Software, Methodology, Investigation, Formal analysis, Data curation, Conceptualization. **Shuang Yang:** Software, Investigation. **Bin-lin Li:** Investigation, Data curation. **Xue Xia:** Software, Investigation. **Wen-bao Jia:** Visualization, Data curation. **Yi-qiao Zhao:** Investigation, Formal analysis. **Ling Lin:** Methodology, Conceptualization. **Jin-lin Bian:** Methodology, Conceptualization. **Tunyaluk Bouphun:** Writing – review & editing. **Wei Xu:** Writing – review & editing, Funding acquisition, Conceptualization.

Declaration of competing interest

The authors declare that they have no known competing financial interests or personal relationships that could have appeared to influence the work reported in this paper.

Data availability

I have shared all data in supplementary material.

Acknowledgments

This work was supported by Sichuan Province S&T Project (2023YFH0025, and 2023YFN0010).

Appendix A. Supplementary data

Supplementary data to this article can be found online at <https://doi.org/10.1016/j.fochx.2024.101969>.

References

- Akiyama, M., Katakura, T., Watanabe, T., Imayoshi, Y., Ikeda, M., Ichihashi, N., ... Iwabuchi, H. (2012). Permeability of volatile compounds from chilled grape-flavored black tea beverage through packaging materials of gable-top cartons.

- Nippon Shokuhin Kagaku Kogaku Kaishi, 59(2), 76–83. <https://doi.org/10.3136/nskkk.59.76>
- Chen, Q., Zhu, Y., Liu, Y., Liu, Y., Dong, C., Lin, Z., & Teng, J. (2022). Black tea aroma formation during the fermentation period. *Food Chemistry*, 374, Article 131640. <https://doi.org/10.1016/j.foodchem.2021.131640>
- Chen, Z., Li, Z., Zhao, Y., Zhu, M., Li, J., & Wang, K. (2024). A meta-analysis of dynamic changes of key aroma compounds during black tea processing. *Food Bioscience*, 58, Article 103784. <https://doi.org/10.1016/j.fbio.2024.103784>
- Denger, K., Smits, T. H. M., & Cook, A. M. (2006). L-Cysteate sulpho-lyase, a widespread pyridoxal 5'-phosphate-coupled desulphonative enzyme purified from *Silicibacter pomeroyi* DSS-3. *The Biochemical Journal*, 394(3), 657–664. <https://doi.org/10.1042/BJ20051311>
- Fitzpatrick, P. F. (2023). The aromatic amino acid hydroxylases: Structures, catalysis, and regulation of phenylalanine hydroxylase, tyrosine hydroxylase, and tryptophan hydroxylase. *Archives of Biochemistry and Biophysics*, 735, Article 109518. <https://doi.org/10.1016/j.abb.2023.109518>
- Huang, W., Fang, S., Wang, J., Zhuo, C., Luo, Y., Yu, Y., Li, L., Wang, Y., Deng, W.-W., & Ning, J. (2022). Sensomics analysis of the effect of the withering method on the aroma components of Keemun black tea. *Food Chemistry*, 395, Article 133549. <https://doi.org/10.1016/j.foodchem.2022.133549>
- Iwamoto, Y., Lee, I. S. M., Kido, R., & Tsubaki, M. (1995). Tryptophan 2,3-dioxygenase in *Saccharomyces cerevisiae*. *Canadian Journal of Microbiology*, 41(1), 19–26. <https://doi.org/10.1139/m95-003>
- Jia, W., Zhao, Y., Liao, S., Li, P., Zou, Y., Chen, S., Chen, W., He, C., Du, X., Zhu, M., & Xu, W. (2022). Dynamic changes in the diversity and function of bacterial community during black tea processing. *Food Research International*, 161, Article 111856. <https://doi.org/10.1016/j.foodres.2022.111856>
- Jiang, B., Yang, L., Luo, X., Huang, R., Jiao, W., Zhong, X., ... Liu, K. (2023). Aroma formation and dynamic changes during Sichuan black tea processing by GC-MS-based metabolomics. *Fermentation*, 9. <https://doi.org/10.3390/fermentation9070686>
- Kavya, D., & Nadumane, V. K. (2023). Enhanced L-Methioninase production by *Methylobacterium* sp. JUBTK33 through RSM and its anticancer potential. *Biocatalysis and Agricultural Biotechnology*, 47, Article 102621. <https://doi.org/10.1016/j.bcab.2023.102621>
- Li, J., & Fitzpatrick, P. F. (2013). Regulation of phenylalanine hydroxylase: Conformational changes upon phosphorylation detected by H/D exchange and mass spectrometry. *Archives of Biochemistry and Biophysics*, 535(2), 115–119. <https://doi.org/10.1016/j.abb.2013.03.006>
- Liang, S., Wang, F., Granato, D., Zhong, X., Xiao, A.-F., Ye, Q., Li, L., Zou, C., Yin, J.-F., & Xu, Y.-Q. (2023). Effect of β -glucosidase on the aroma of liquid-fermented black tea juice as an ingredient for tea-based beverages. *Food Chemistry*, 402, Article 134201. <https://doi.org/10.1016/j.foodchem.2022.134201>
- Liu, C., Lin, H., Wang, K., Zhang, Z., Huang, J., & Liu, Z. (2023). Study on the trend in microbial changes during the fermentation of black tea and its effect on the quality. *Foods*, 12(10), 1944. <https://doi.org/10.3390/foods12101944>
- Liu, S., Li, T., Yu, S., Zhou, X., Liu, Z., Zhang, X., Cai, H., & Hu, Z. (2023). Analysis of bacterial community structure of Fuzhuan tea with different processing techniques. *Open Life Sciences*, 18(1), Article 20220573. <https://doi.org/10.1515/biol-2022-0573>
- Logue, J. B., Stedmon, C. A., Kellerman, A. M., Nielsen, N. J., Andersson, A. F., Laudon, H., ... Kritzbeg, E. S. (2016). Experimental insights into the importance of aquatic bacterial community composition to the degradation of dissolved organic matter. *The ISME Journal*, 10(3), 533–545. <https://doi.org/10.1038/ismej.2015.131>
- Mo, X.-H., Sun, Y.-M., Bi, Y.-X., Zhao, Y., Yu, G.-H., Tan, L., & Yang, S. (2023). Characterization of C30 carotenoid and identification of its biosynthetic gene cluster in *Methylobacterium extorquens* AM1. *Synthetic and Systems Biotechnology*, 8(3), 527–535. <https://doi.org/10.1016/j.synbio.2023.08.002>
- Nurmilah, S., Cahyana, Y., & Utama, G. L. (2022). Metagenomics analysis of the polymeric and monomeric phenolic dynamic changes related to the indigenous bacteria of black tea spontaneous fermentation. *Biotechnology Reports*, 36, Article e00774. <https://doi.org/10.1016/j.btre.2022.e00774>
- Parke, D. (1996). Conservation of PcaQ, a transcriptional activator of pca genes for catabolism of phenolic compounds, in *Agrobacterium tumefaciens* and *Rhizobium* species. *Journal of Bacteriology*, 178(12), 3671–3675. <https://doi.org/10.1128/jb.178.12.3671-3675.1996>
- Phillips, R. S., Crocker, M., Lin, R., Idowu, O. E., McCannan, D. K., & Lima, S. (2019). The roles of Ser-36, Asp-132 and Asp-201 in the reaction of *Pseudomonas fluorescens* Kynureninase. *Biochimica et Biophysica Acta (BBA) - Proteins and Proteomics*, 1867(7–8), 722–731. <https://doi.org/10.1016/j.bbapap.2019.05.005>
- Qu, T., Wang, P., Zhao, X., Liang, L., Ge, Y., & Chen, Y. (2024). Metagenomics reveals differences in the composition of bacterial antimicrobial resistance and antibiotic resistance genes in pasteurized yogurt and probiotic bacteria yogurt from China. *Journal of Dairy Science*, Article S0022030224000225. <https://doi.org/10.3168/jds.2023-23983>
- Ren, Z.-W., Pan, H.-J., Hu, C., Le, M.-M., Long, Y.-H., Xu, Q., Xie, Z.-W., & Ling, T.-J. (2024). Rolling forms the diversities of small molecular nonvolatile metabolite profile and consequently shapes the bacterial community structure for Keemun black tea. *Food Research International*, 181, Article 114094. <https://doi.org/10.1016/j.foodres.2024.114094>
- Sabrialabed, S., Yang, J. G., Yariv, E., Ben-Tal, N., & Lewinson, O. (2020). Substrate recognition and ATPase activity of the *E. coli* cysteine/cystine ABC transporter YecSC-FlY. *Journal of Biological Chemistry*, 295(16), 5245–5256. <https://doi.org/10.1074/jbc.RA119.012063>
- Sun, Z., Lin, Y., Yang, H., Zhao, R., Zhu, J., & Wang, F. (2024). Characterization of honey-like characteristic aroma compounds in Zunyi black tea and their molecular mechanisms of interaction with olfactory receptors using molecular docking. *LWT*, 191, Article 115640. <https://doi.org/10.1016/j.lwt.2023.115640>
- Thackray, S. J., Mowat, C. G., & Chapman, S. K. (2008). Exploring the mechanism of tryptophan 2,3-dioxygenase. *Biochemical Society Transactions*, 36(6), 1120–1123. <https://doi.org/10.1042/BST0361120>
- Thomas, D., Barbey, R., & Surdin-Kerjan, Y. (1993). Evolutionary relationships between yeast and bacterial homoserine dehydrogenases. *FEBS Letters*, 323(3), 289–293. [https://doi.org/10.1016/0014-5793\(93\)81359-8](https://doi.org/10.1016/0014-5793(93)81359-8)
- Tong, W., Yu, J., Wu, Q., Hu, L., Tabys, D., Wang, Y., ... Bennetzen, J. L. (2021). Black tea quality is highly affected during processing by its leaf surface microbiome. *Journal of Agricultural and Food Chemistry*, 69(25), 7115–7126. <https://doi.org/10.1021/acs.jafc.1c01607>
- Wang, A., Lei, Q., Zhang, B., Wu, J., Fu, Z., He, J., Wang, Y., & Wu, X. (2024). Revealing novel insights into the enhancement of quality in black tea processing through microbial intervention. *Food Chemistry: X*, 23, Article 101743. <https://doi.org/10.1016/j.fochx.2024.101743>
- Wang, M.-Q., Ma, W.-J., Shi, J., Zhu, Y., Lin, Z., & Lv, H.-P. (2020). Characterization of the key aroma compounds in Longjing tea using stir bar sorptive extraction (SBSE) combined with gas chromatography-mass spectrometry (GC-MS), gas chromatography-olfactometry (GC-O), odor activity value (OAV), and aroma recombination. *Food Research International*, 130, Article 108908. <https://doi.org/10.1016/j.foodres.2019.108908>
- Wu, W., Jiang, X., Zhu, Q., Yuan, Y., Chen, R., Wang, W., Liu, A., Wu, C., Ma, C., Li, J., Zhang, J., & Peng, Z. (2024). Metabonomics analysis of the flavor characteristics of Wuyi Rock Tea (Rougui) with “rock flavor” and microbial contributions to the flavor. *Food Chemistry*, 450, Article 139376. <https://doi.org/10.1016/j.foodchem.2024.139376>
- Yang, Y., Wang, Q., Xie, J., Deng, Y., Zhu, J., Xie, Z., ... Jiang, Y. (2024). Uncovering the dynamic alterations of volatile components in sweet and floral aroma black tea during processing. *Foods*, 13(5), 728. <https://doi.org/10.3390/foods13050728>
- Yang, Y., Xie, J., Wang, Q., Deng, Y., Zhu, L., Zhu, J., Yuan, H., & Jiang, Y. (2024). Understanding the dynamic changes of volatile and non-volatile metabolites in black tea during processing by integrated volatilomics and UHPLC-HRMS analysis. *Food Chemistry*, 432, Article 137124. <https://doi.org/10.1016/j.foodchem.2023.137124>
- Yang, Z., Baldermann, S., & Watanabe, N. (2013). Recent studies of the volatile compounds in tea. *Food Research International*, 53(2), 585–599. <https://doi.org/10.1016/j.foodres.2013.02.011>
- Yao, H., Su, H., Ma, J., Zheng, J., He, W., Wu, C., Hou, Z., Zhao, R., & Zhou, Q. (2023). Widely targeted volatilomics analysis reveals the typical aroma formation of Xinyang black tea during fermentation. *Food Research International*, 164, Article 112387. <https://doi.org/10.1016/j.foodres.2022.112387>